

rotation is used, as evidenced from Figure 5. In the case of scanning in the azimuth plane, the pattern shape is relatively well-preserved irrespective of the type of subreflector movement, as expected from the proximity of the curves in Figure 4.

ACKNOWLEDGMENT

The initial portion of this work was done (using the code GRASP8) while the second author was at COMDEV Ltd. The majority of the work was completed at the University of Ottawa (using GRASP8W Student Edition).

REFERENCES

1. K.W. Brown and A. Prata, A design procedure for classical offset dual reflector antennas with circular apertures, *IEEE Trans Antennas Propagat AP-42* (1994), 1145–1152.
2. A.W. Rudge et al. (Ed.), *The handbook of antenna design*, vol. II, Peter Peregrinus, Ltd., London, 1983, pp. 136–142.
3. A.V. Mrstik, Scan limits of off-axis fed parabolic reflectors, *IEEE Trans Antennas Propagat AP-27* (1979), 647–651.
4. Y. Rahmat-Samii and V. Galindo-Israel, Scan performance of dual offset reflector antennas for satellite communications, *Radio Sci* 16 (1981), 1093–1099.
5. V. Krichevsky, Beam scanning in offset Cassegrain antenna, *IEEE AP-S Int Symp Dig 1* (1982), 257–260.
6. D.C.D. Chang and K.C. Lang, Preliminary study on offset scan-corrected reflector antenna system, *IEEE Trans Antennas Propagat AP-32* (1984), 30–35.
7. A.R. Dion and L.V. Muresan, Electromagnetic scattering by arbitrarily shaped reflectors: Subreflector efficiency, *IEEE Trans Antennas Propagat AP-33* (1985), 1338–1346.
8. Y. Rahmat-Samii, Subreflector extension for improved efficiencies in Cassegrain antennas: GTD/PO analysis, *IEEE Trans Antennas Propagat AP-34* (1986), 1266–1269.
9. V. Galindo-Israel, W. Verrutpong, R.D. Norrod, and W.A. Imbriale, Scanning properties of large dual-shaped offset and symmetric reflectors, *IEEE Trans Antennas Propagat AP-40* (1992), 422–432.
10. W.V.T. Rusch and A.C. Ludwig, Determination of the maximum scan-gain contours of a beam-scanning paraboloid and their relation to the Petzval surface, *IEEE Trans Antennas Propagat AP-21* (1973), 141–147.
11. C.J. Sletten, Focal surfaces of offset dual-reflector antennas, *IEE Proc* 129 H (1982), 109–115.
12. V. Krichevsky and D.F. DiFonzo, Optimum beam scanning in offset single and dual reflector antennas, *IEEE Trans Antennas Propagat AP-33* (1985), 179–188.
13. R. Mizzoni and R. Jorgensen, A novel elliptical spot beam antenna with beam reconfiguration capability, *IEEE AP-S Symp Dig* (1998), Atlanta, GA, 824–827.
14. R. Jorgensen and R. Mizzoni, Gregorian antennas with limited beam reconfiguration and steering capability, *Proc Millenn Conf Antennas Propagat*, Davos, Switzerland, April 2004.
15. Code GRASP8, TICRA Engineering Consultants, Denmark, www.ticra.com.
16. Code GRASP8W Student Edition, TICRA Engineering Consultants, Denmark, www.ticra.com.
17. Code REFLECT, Antenna Software Limited, UK, www.demon.co.uk/asl.
18. K. Pontoppidan (Ed.), Technical description of GRASP8, www.ticra.com, TICRA Engineering Consultants, Copenhagen, Denmark. See also *IEEE Antennas Propagat Mag* 44 (2002), 125–126.
19. V. Jamnejad-Dailami and Y. Rahmat-Samii, Some important geometrical features of conic-section generated offset reflector antennas, *IEEE Trans Antennas Propagat AP-28* (1980), 952–957.
20. Y. Rahmat-Samii, Useful coordinate transformations for antenna applications, *IEEE Trans Antennas Propagat AP-27* (1979), 571–574.
21. C. Granet, Designing classical offset Cassegrain or Gregorian dual-reflector antennas from combinations of prescribed geometrical parameters, *IEEE Antennas Propagat Mag* 44 (2002), 114–123.

© 2005 Wiley Periodicals, Inc.

ALL-OPTICAL HEADER PROCESSING USING AN INJECTION-LOCKED FABRY-PÉROT LASER DIODE

L. Y. Chan,¹ P. K. A. Wai,¹ L. F. K. Lui,¹ Lixin Xu,¹ H. Y. Tam,² and M. S. Demokan²

¹ Photonics Research Centre and Dept. of Electronic and Information Engineering

The Hong Kong Polytechnic University
Hong Kong, China

² Photonics Research Centre and Dept. of Electrical Engineering
The Hong Kong Polytechnic University
Hong Kong, China

Received 22 July 2004

ABSTRACT: Simultaneous all-optical header processing and control packet switching are demonstrated by using multiwavelength injection-locking in a single Fabry-Pérot laser diode. A special two-level control packet is used to process the header of the data packet at 5 Gb/s. The entire control packet is all optically switched ON or OFF. © 2005 Wiley Periodicals, Inc. *Microwave Opt Technol Lett* 44: 342–345, 2005; Published online in Wiley InterScience (www.interscience.wiley.com). DOI 10.1002/mop.20629

Key words: all-optical devices; all-optical header processing; all-optical packet switching; Fabry-Pérot laser; injection-locking

1. INTRODUCTION

All-optical packet switching is one of the key enabling technologies for future broadband networks. In true all-optical switching, both header processing and packet switching are carried out in the optical domain, thus eliminating the need for opto-electronic conversion. A variety of header-processing schemes have been demonstrated using nonlinear optical loop mirror [1–3]. Hill et al. implemented a 1×2 all-optical switch using two-pulse correlation principle in a semiconductor laser amplifier in a loop optical mirror (SLALOM) configuration [4–5]. The data rate of the packet payload is 2.5 Gb/s with the header length of the order of microseconds. In this paper, we demonstrate simultaneous all-optical processing of the data-packet headers and switching of the control packets for data packets with payload rate of 10 Gb/s and header rate of 5 Gb/s using multiwavelength mutual injection-locking in a Fabry-Pérot laser diode (FP-LD). The header processing is achieved using a special control packet by which the outcome of the optical processing of one bit in the data-packet header will switch the entire control packet ON or OFF. The switched control packets' output can then be used to switch the data packets ON or OFF, for example, again using multiwavelength mutual injection-locking in a FP-LD, as described [6].

2. OPERATION PRINCIPLE

We utilize the multimode injection locking property and the bistable characteristic of injection-locking in an injection-locked FP-LD for all-optical header processing and switching of the control packet. The header processing is based on the observation that the presence of a signal at a wavelength λ_d of a FP-LD can lower the injection-locking threshold at another wavelength λ_c . The switching of the control packets makes use of the bistable nature of injection-locking in FP-LDs, that is, it takes less power to maintain injection-locking than to initiate one. Figure 1 shows the input-output power characteristic of a continuous wave (CW)

Lixin Xu is on leave from the Department of Physics, University of Science and Technology of China, Hefei, 230026, China.

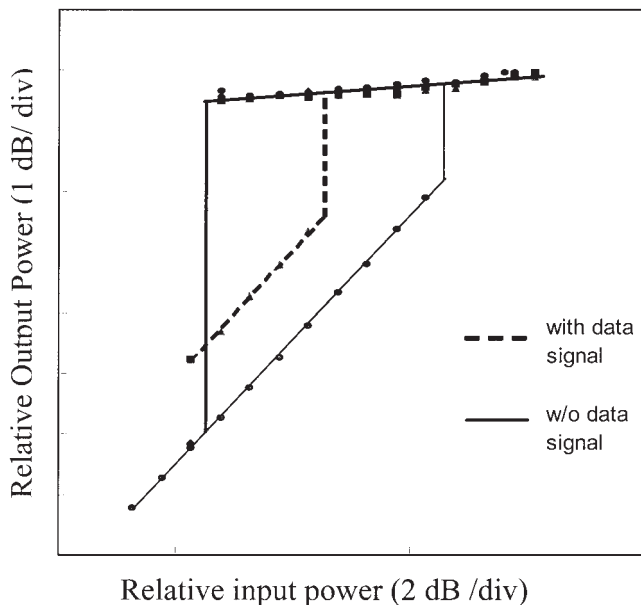


Figure 1 Input/output power characteristics for the CW control signal at 1547.02 nm under one-mode and two-mode injection-locking in an FP-LD (solid and dashed lines give the hysteresis curves without and with the presence of the data signal at 1554.60 nm with a power of -10 dBm, respectively)

signal injected into a FP-LD under one-mode and two-mode injection. The CW signal is generated from a tunable laser at a wavelength of 1547.02 nm with $+0.1$ -nm-wavelength detuned from one of the free-running longitudinal modes of a commercially available FP-LD biased at $1.3 I_{th}$, where I_{th} is the threshold current. The solid lines show the power hysteresis of single-mode injection locking. We observed that the power required to maintain injection-locking of an FP-LD can be less than the power required to initiate injection-locking from its unlocked state. The dashed line in Figure 1 shows the measured hysteresis of the same injected signal when a second signal at 1554.60 nm, which is at zero detune from another FP-LD mode, is injected into the FP-LD at a power

of -10 dBm. Note that the injection-locking threshold of the first injected signal decreases in the presence of the second signal.

Figure 2 illustrates the proposed scheme for all-optical header processing and control-packet switching using a single FP-LD. The proposed scheme requires a special control packet at wavelength λ_c that has a trigger at power P_H and a long trailer at power P_T , where $P_H > P_T$ [Fig. 2(a)]. The guard band between the control packets is at zero power. Ideally, the width of the trigger should equal to the bit period of the data-packet payload. The total length of the control packet is equal to that of the data packet. The wavelengths of the control packets and data packets, λ_c and λ_d , are located at the longer wavelength side of two different longitudinal modes of the FP-LD. The power of the control packet trigger P_H is chosen to be $P_{th2} \leq P_H < P_{th1}$, where P_{th1} and P_{th2} are the injection-locking thresholds of the FP-LD at λ_c in the absence and presence of the data signal at λ_d , respectively. In other words, P_{th1} and P_{th2} are the respective single-mode and dual-mode injection-locking thresholds of the FP-LD at λ_c . Thus, the control-packet trigger will injection-lock the FP-LD and experience power gain if it matches a '1' in the data signal, but the control-packet trigger cannot initiate injection locking alone, that is, if it matches with a '0' in the data signal. The power of the control packet trailer P_T is chosen to be $P_{th3} \leq P_T < P_{th2}$, where P_{th3} is the power at which the FP-LD returns to the unlocked state from the locked state, such that once the control-packet trigger initiates injection-locking in the FP-LD, the trailer can sustain the injection-locking up to the end of the control packet due to the bistable property of injection-locking. The control packet trailer, however, cannot initiate injection-locking, even in the presence of the '1' bits in the data packet. From Figure 1, P_{th3} at λ_c is the same in either the presence or absence of the signal at λ_d . Figure 2(b) schematically shows the control packet at the output of the FP-LD without (grey region) and with (dashed lines) injection locking. Figure 2(c) shows how the proposed header processor and control-packet switching work schematically. For packet 1, the control-packet trigger matches with the '1' bit in the header in the time domain. Injection-locking at λ_c is initiated and sustained through the duration of the control packet. The output of the FP-LD at λ_c is therefore high (ON state). For packet 2, the control-packet trigger does not match with the '1' bit in the header. Injection locking at λ_c is not initiated either at the

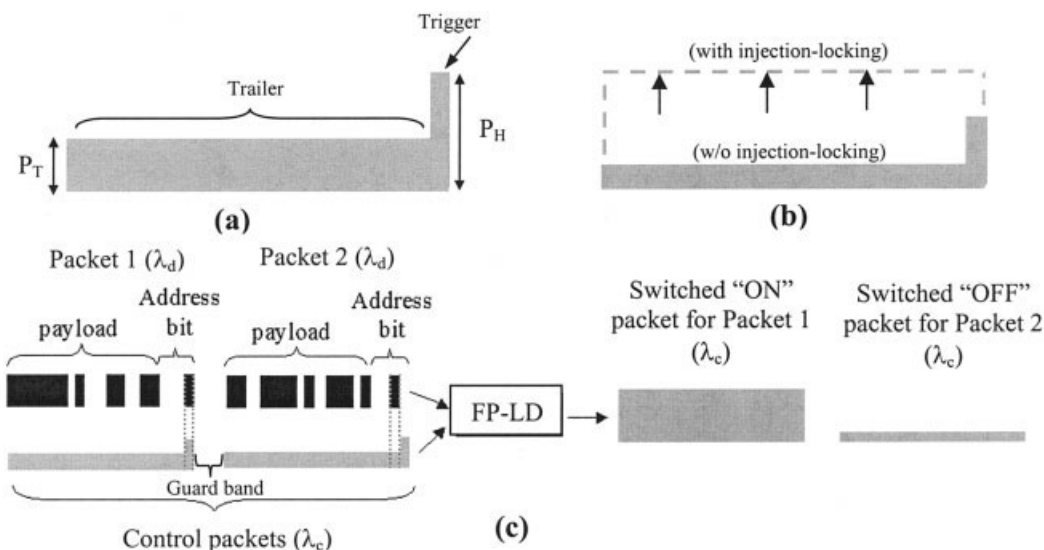


Figure 2 Schematics of the (a) proposed format of the control packet, (b) output of the control packets with (dashed lines) and without (grey) injection-locking by the triggering header, and (c) all-optical switching of the control packets with all-optical header processing

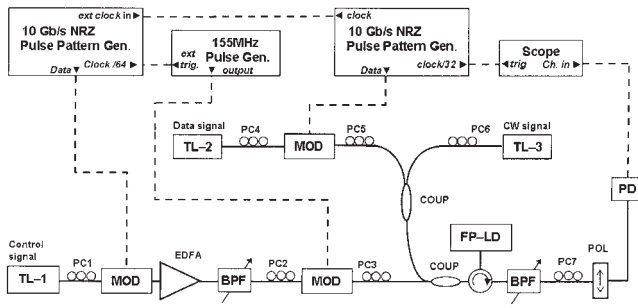


Figure 3 Experimental setup (TL: tunable laser, PC: polarization controller, MOD: modulator, COUP: intensity coupler, CIR: circulator, FP-LD: Fabry-Pérot laser diode, BPF: variable bandpass filter, EDFA: erbium-doped fibre amplifier, POL: polarizer, PD: photodiode)

control-packet trigger or at another part of the control packet. The output of the FP-LD at λ_c is low (OFF state). Since the switching action is completely determined by the optical processing of a single bit in the header of the data packet, the proposed scheme can be used to implement a recently proposed self-routing address format for all-optical packet switched networks with arbitrary topologies [7].

3. EXPERIMENTAL RESULTS

Figure 3 shows the experimental setup for the proposed all-optical header processing scheme. A CW signal at 1537.41 nm with power of -11.98 dBm (measured before injection into the FP-LD) from a tunable laser (TL-3) is injected into the main mode of the FP-LD in order to suppress the output of the FP-LD during the guard band period. The 10-Gb/s non-return-to-zero (NRZ) data packet at 1534.65 nm was generated by externally modulating a tunable laser (TL-2) with power of -20.35 dBm (measured before injection into the FP-LD). The control signal at 1541.41 nm was produced by externally modulating another tunable laser (TL-1) using two Mach-Zehnder modulators with different extinction ratios [8]. The power for the control packet measured at the output of the FP-LD is -1.83 dBm before injection into the FP-LD. The pulsewidth of the trigger in the control packet is 200 ps, which determines the header processing rate as 5 Gb/s. The duration of the control packet is 5.5 ns and the guard period is 0.95 ns; thus, the repetition rate is 155 MHz. The wavelength detunes for the control packets, the input data packets and the CW signal are $+0.24$ nm, $+0.08$ nm, and $+0.06$ nm with three different FP-LD modes, respectively. The bias current of the FP-LD was $1.3 I_{th}$. Figure 4(a) shows the temporal profile of the control packet. Figures 4(b) and 4(c) shows the two types of data packets used: packet 1 and packet 2, which have a 2-bit address with bit patterns of '10' and '01', respectively. The bit period is 200 ps, and thus the header rate is 5 Gb/s. The payload rate is 10 Gb/s. We synchronized the input data packets and the control packets such that the headers of the data packets are aligned with the control packet trigger. Figures 5(a), 5(b), and 5(c) show the input 10-Gb/s NRZ data packets, the synchronized input control packet, and the switched output of the control packets, respectively. We observed that the output of the control packet is high (ON) and low (OFF) if the control packet trigger matches with a '1' or '0' bit, respectively, in the data-packet address header. Figure 6 depicts the spectrum of the multiwavelength injection-locked FP-LD. The output of the proposed header processor can be injected into the all-optical switch, as demonstrated in [6], in order to switch the data packet.

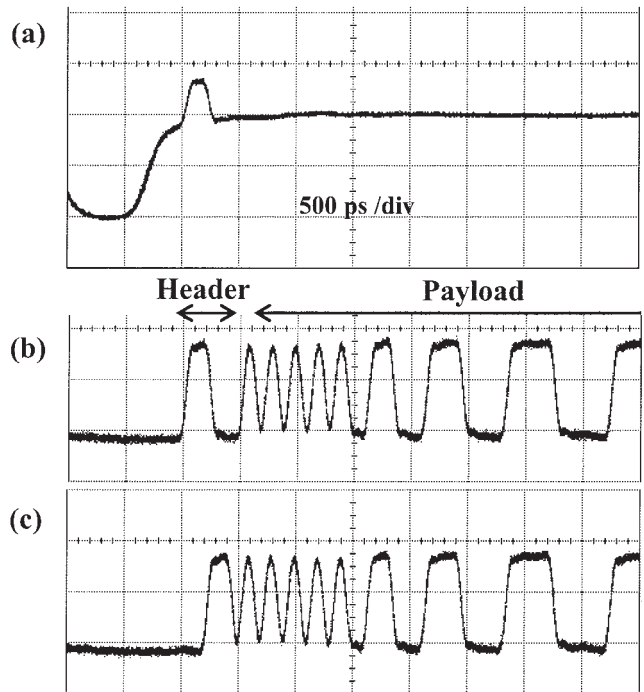


Figure 4 Temporal profiles for the (a) control packet with 200-ps header and a repetition rate of 155 MHz, (b) input data packet with 10-Gb/s payload and 5-Gb/s header with head bit pattern '10' (packet 1), and (c) '01' (packet 2)

4. CONCLUSION

In conclusion, we have demonstrated an all-optical header processor and switching of the control packet by using a multiwavelength injection-locked FP-LD with a specially designed dual-level con-

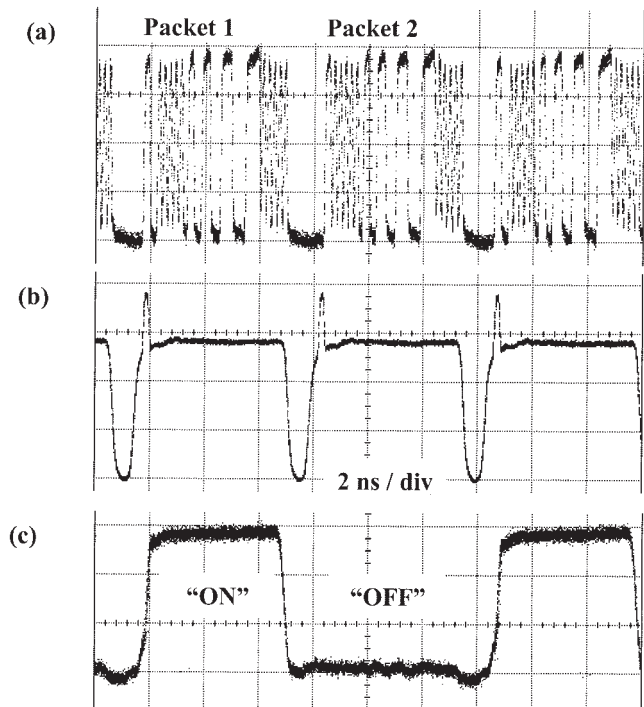


Figure 5 Temporal profiles for (a) input data packets (packets 1 and 2), (b) input control packet with a 200-ps header (trigger) and a repetition rate of 155 MHz, and (c) switched control packets at the output of the FP-LD (packet 1 is switched ON while packet 2 is switched OFF)

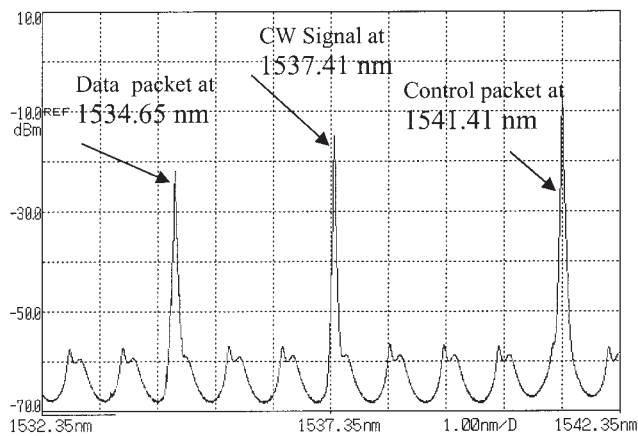


Figure 6 Spectrum for the multiwavelength injection-locked FP-LD

control packet. The header-processing speed is 5 Gb/s while the payload data rate is 10 Gb/s. A single bit in the header of the data packet determines whether the control packet will be switched ON or OFF at the output of the FP-LD.

ACKNOWLEDGMENT

P. K. A. Wai acknowledges the support of the Research Grant Council of the Hong Kong Special Administrative Region, China, under project no. PolyU5242/03E.

REFERENCES

1. J.P. Sokoloff, P.R. Prucnal, I. Glesk, and M. Kane, A terahertz optical asymmetric demultiplexer (TOAD), *IEEE Photon Technol Lett* 5 (1993), 787–790.
2. C. Schunert, J. Berger, S. Diez, H.J. Ehrke, R. Ludwig, U. Feiste, C. Schmidt, H.G. Weber, G. Toptchiyski, S. Randel, and K. Petermann, Comparison of interferometric all-optical switches for demultiplexing applications in high-speed OTDM systems, *J Lightwave Technol* 20 (2002), 618–624.
3. H.C. Lim, T. Sakamoto, and K. Kikuchi, Polarization-independent optical demultiplexing by conventional nonlinear optical loop mirror in a polarization-diversity loop configuration, *IEEE Photon Technol Lett* 12 (2000), 1704–1706.
4. M.T. Hill, A. Srivatsa, N. Calabretta, Y. Liu, H. de Waardt, G.D. Khoe, and H.J.S. Dorren, 1×2 optical packet switch using all-optical header processing, *Electron Lett* 37 (2001), 774–775.
5. H.J.S. Dorren, M.T. Hill, Y. Liu, N. Calabretta, A. Srivatsa, F.M. Huijskens, H. de Waardt, and G.D. Khoe, Optical packet switching and buffering by using all-optical signal processing methods, *J Lightwave Technol* 21 (2003), 2–12.
6. L.Y. Chan, P.K.A. Wai, L.F.K. Lui, B. Moses, W.H. Chung, H.Y. Tam, and M.S. Demokan, Demonstration of an all-optical switch by use of a multiwavelength mutual injection-locked laser diode, *Optics Lett* 28 (2003), 837–839.
7. X.C. Yuan, V.O.K. Li, C.Y. Li, and P.K.A. Wai, A novel self-routing address scheme for all-optical packet-switched networks with arbitrary topologies, *J Lightwave Technol* 21 (2003), 329–339.
8. L.Y. Chan, K.K. Qureshi, P.K.A. Wai, B. Moses, L.F.K. Lui, H.Y. Tam, and M.S. Demokan, All-optical bit-error monitoring system using cascaded inverted wavelength converter and optical NOR gate, *IEEE Photon Technol Lett* 15 (2003), 593–595.

NUMERICAL ANALYSES OF TENS-OF-GIGAHERTZ PULSE-SIGNAL GENERATION USING A SIDEBAND INJECTION-LOCKING SCHEME

Jung-Tae Kim

Department of Electronic & Information Security Engineering
Mokwon University
800, Doan-Dong
Seogu, Daejeon, 302-729, Korea

Received 22 July 2004

ABSTRACT: We analyze tens-of-gigahertz pulse signal generation using a sideband injection-locking scheme. The numerical model for semiconductor lasers under the external optical injection is based on Lang's equation and has been extended in order to take into account the simultaneous injection of the multiple sidebands of the current-modulated laser. The numerical-simulation results show that the unselected sidebands will affect the optical and RF-spectral characteristics, even though the semiconductor laser is locked to the target sidebands. The simulation results are confirmed by the experimental results. © 2005 Wiley Periodicals, Inc. *Microwave Opt Technol Lett* 44: 345–348, 2005; Published online in Wiley InterScience (www.interscience.wiley.com). DOI 10.1002/mop.20630

Key words: heterodyne scheme; injection locking; millimeter-wave signal generation

1. INTRODUCTION

The optical injection-locking technique with semiconductor laser diodes (LDs) is widely used in chirp and linewidth reduction, measurement of the laser dynamics, wavelength conversion, and optical-microwave generation. In particular, the optical-microwave signal-generation technique using injection-locked lasers is very promising for many applications because it can easily produce high-frequency signals with low phase noise. In the sideband injection-locking scheme, the master laser (ML) is electrically modulated and two of the resultant sidebands having the desired frequency separation are injected into two slave lasers (SLs) [1]. When these two injection-locked SLs beat each other in the photodiode (PD), the desired microwave signal is generated. Using this method, Braun et al. have recently reported the successful demonstration of 60-GHz beat-signal generation [2]. Our recent study on FM sideband injection-locking has shown that when SLs are locked to the target sidebands of the directly modulated ML, the presence of the unselected sidebands influences the resultant microwave signals. The unselected sidebands can produce unwanted beat signals around the desired beat signal, which degrade the overall system performance. The reduction of incident light power helps to suppress the unwanted beat signals, but it also reduces the locking range, thus causing the stability problem. In this paper, we investigate tens-of-gigahertz pulse-signal generation using heterodyne scheme in numerical and experimental methods. The numerical models for the sideband injection-locked SLs are based on the extended Lang's model, which includes the influence of multiple ML sidebands expressed by the Bessel function [3]. With multiple ML sidebands, the large-signal analyses for the SL spectra are performed. Finally, we investigate the influence of the unselected sidebands on the SL spectral properties for different ML injection powers.